Photoemission and x-ray absorption study of superconducting and semiconducting $Ba_{1-x}K_xBiO_3$ single crystals

M. Qvarford
Department of Synchrotron Radiation Research, Institute of Physics, Lund University, Box 118, S-221 00 Lund, Sweden

V. G. Nazin, A. A. Zakharov, and M. N. Mikheeva
Russian Research Center ''Kurchatov Institute,'' Kurchatov Square 1, 123182 Moscow, Russia

J. N. Andersen, M. K.-J. Johansson, and G. Chiaia*
Department of Synchrotron Radiation Research, Institute of Physics, Lund University, Box 118, S-221 00 Lund, Sweden

T. Rogelet, S. Söderholm, and O. Tjernberg
Materials Physics, Department of Physics, Royal Institute of Technology, S-100 44 Stockholm, Sweden

H. Nylén, I. Lindau, and R. Nyholm
Department of Synchrotron Radiation Research, Institute of Physics, Lund University, Box 118, S-221 00 Lund, Sweden

U. O. Karlsson
Materials Physics, Department of Physics, Royal Institute of Technology, S-100 44 Stockholm, Sweden

S. N. Barilo and S. V. Shiryaev
Institute of Solid State Physics and Semiconductors, 220072 Minsk, Belorussia

(Received 8 March 1996)

Semiconducting $Ba_{0.9}K_{0.1}BiO_3$ and superconducting $Ba_{0.6}K_{0.4}BiO_3$ single crystals cleaved *in situ* have been studied by core level and valence band photoelectron spectroscopy and O K edge x-ray absorption spectroscopy. It was found that the general shape of the valence band spectrum agrees with the shape predicted by band structure calculations, but the intensity near the Fermi level was lower in the experimental spectrum as compared to the calculated. The O K edge spectra showed that the metallic phase is not related to the presence of doping inducted O $2p$ holes. This property of $Ba_{1-x}K_xBiO_3$ shows that the semiconductor-metal transition of this system is of a different nature than that of the hole doped cuprate high-T_c superconductors. The core level photoemission spectra of the cations showed a small asymmetry for $Ba_{0.9}K_{0.1}BiO_3$. Corresponding spectra for $Ba_{0.6}K_{0.4}BiO_3$ showed a larger asymmetry resulting in a resolved high binding energy shoulder in the Bi $4f$ spectrum. The origin of this feature is discussed. [S0163-1829(96)01333-1]

I. INTRODUCTION

A common property of most high-T_c superconductors (HTSC) is the presence of Cu-O_2 layers in their lattice. Band-structure calculations predict these materials to have dispersive Cu-O bands at the Fermi level (E_F).[1] $Ba_{1-x}K_xBiO_3$ is a high-T_c oxide superconductor system which has no Cu-O_2 layers in the lattice.[2] The highest T_c, about 30 K, is obtained for $x=0.4$.[3] This composition gives a cubic perovskite crystal structure,[3] a structure clearly different from the layered two-dimensional structures typical for the cuprate HTSC. Band-structure calculations[4–6] predict that a dispersive Bi-O band crosses the Fermi level, i.e., in this material the Bi atoms are regarded to play the role of the Cu atoms in the cuprate HTSC. Strong electron correlation which is known to be crucial for cuprate HTSC is not expected in the $Ba_{1-x}K_xBiO_3$ system since the valence band is predicted to contain only s and p states. These differences between $Ba_{1-x}K_xBiO_3$ and the cuprate HTSC may imply that also the mechanism for superconductivity is different.

In order to experimentally investigate possible differences and similarities in the electronic structure of $Ba_{1-x}K_xBiO_3$ and the cuprate HTSC, electron spectroscopy studies are of great importance. One main goal for such studies is to elucidate the physics behind the potassium-induced transition from a semiconductor ($x<0.3$) to a metal ($x>0.3$).[7] This transition coincides with a crystallographic phase transition between cubic and distorted structures, the metallic phase being cubic and the semiconducting phase monoclinic ($0\leqslant x<0.1$) or orthorhombic ($0.1<x<0.3$), depending on the value of x.[7] It has been shown that the structures of the semiconducting phase contain two inequivalent Bi sites.[8] Several photoemission[9–16] and x-ray-absorption[8] (XAS) studies of the $Ba_{1-x}K_xBiO_3$ (or the similar $Ba_{1-x}Rb_xBiO_3$) system have been performed. Among these, several controversial questions have emerged for which the answers deviate from study to study. For instance, different interpretations have been proposed[9,11,14,15] for the Bi $4f$ and O $1s$ core-level data in terms of the number of chemically shifted components corresponding to inequivalent sites and/or oxidation states. In the reported valence-band data there is a growing consensus that superconducting

samples give a clear Fermi edge[9,11,13,15,16] which is lacking for the semiconducting compositions,[9,13,15,16] but in two studies[12,14] no clear Fermi edge was found for superconducting samples. All studies except one[16] were performed with polycrystalline samples and scraping was the most frequently used method to clean the surface.

An important question in this context is how a nonstoichiometric or contaminated sample surface may influence the spectra. It can, for instance, have an effect on the shape of the O 1*s* core-level spectrum as well as on the intensity distribution in the valence-band region. It is especially important to investigate if the intensity at E_F is affected by the surface quality. Furthermore, it must be realized that the cleaning procedure used, for instance scraping, may be hazardous for the surface stoichiometry. In the work by Nagoshi *et al.*[15] it was shown that scraping can diminish the photoemission intensity in the vicinity of E_F. In addition, Bi core-level photoemission spectra have shown that scraping can result in breaking of the Bi-O bonds.[12] Concerning the reactivity of the surfaces in ultrahigh vacuum (UHV) it has been concluded that the absorption of residual gas molecules is larger for potassium doped samples.[11]

The present work is a photoemission and XAS study of $Ba_{1-x}K_xBiO_3$ single crystals which were cleaved *in situ*. Careful attention was paid to the cleanliness of the crystal surfaces as revealed by the C 1*s*, O 1*s*, and valence-band photoemission spectra in order to distinguish between extrinsic and intrinsic spectral features. The samples were cooled by liquid nitrogen in order to diminish possible oxygen desorption and chemical reaction at the surface. Moreover, the measurements were done with a high-energy resolution which made it possible to resolve features in core-level spectra not reported previously. Two different compositions, representing different parts of the $Ba_{1-x}K_xBiO_3$ phase diagram, have been compared: semiconducting $Ba_{0.9}K_{0.1}BiO_3$ and superconducting $Ba_{0.6}K_{0.4}BiO_3$. The measurements comprise core-level photoemission of all constituents, valence-band photoemission and O *K*-edge XAS, and were performed with synchrotron radiation as the photon source.

The results are presented and discussed in Sec. III which is divided into three parts. In Sec. III A the core-level photoemission spectra are treated. The O 1*s* spectra are discussed with the emphasis on how they can be affected by contamination. The core-level data for clean samples show that the line shapes for $Ba_{0.6}K_{0.4}BiO_3$ are more complicated than what could be expected from the cubic structure. Section III B deals with the valence-band photoemission data which are compared to the predictions from band-structure calculations. In general, the agreement is found to be good. Finally, in Sec. III C the O *K*-edge XAS spectra are discussed and their doping dependence is compared to what is known for the cuprate HTSC. It is argued that the metallic properties of $Ba_{0.6}K_{0.4}BiO_3$ cannot be related to the presence of doping induced oxygen holes as is the case for the hole-doped cuprate HTSC.

II. EXPERIMENT

$Ba_{1-x}K_xBiO_3$ single crystals were grown from a KOH fluxed melt employing the electrodeposition technique introduced by Norton.[17] A controlled anode current density was used. The as-grown crystals were close to cubic in shape and the average dimension of the crystals grown for 60–100 h was $3\times3\times3$ mm^3. The crystals were examined by neutron diffraction and the block disorientation angle within the crystals was found to be less than 1.5°. Potassium content was determined by three different methods: (i) by using a calibration curve for pseudocubic lattice parameter vs potassium concentration,[7] (ii) by measuring the natural radioactivity of potassium, the ^{40}K isotope, and (iii) by neutron activation analyses. The values obtained by the natural radioactivity and neutron activation methods, i.e., the direct methods, $x=0.11$ and 0.4, will be used in the following. Using the first method, x-ray-diffraction measurements gave slightly higher potassium concentrations (up to 20%).

The critical temperature of superconducting samples ($x=0.4$) was determined by using both four probe resistivity as well as ac susceptibility measurements. Both methods gave a sharp transition with $T_c=15$ K defined as the midpoint of the transition. It has been found that T_c of $Ba_{1-x}K_xBiO_3$ is not only dependent on the amount of potassium, but is also strongly dependent on small changes in the oxygen content.[18,19] This property probably explains the low T_c, as compared to the optimum value 30 K,[3] for the present $Ba_{0.6}K_{0.4}BiO_3$ crystals. The temperature (T) dependence of the resistivity for the superconducting samples above T_c is very close to $\rho=\rho_0+aT^2$ (a is a constant), in agreement with previous measurements.[20]

The crystals were glued with conducting silver epoxy to sample holders made of copper with the naturally formed {100} plane of the crystals as base. For cleavage a metal stick was glued to the top of the crystals. The samples were transferred into the baked UHV chamber where they were cleaved by fracturing at a pressure around 10^{-10} Torr. The fracturing was performed by applying a sudden force to the metal stick. The surfaces of the fractured samples were rough but shining, brown for $Ba_{0.9}K_{0.1}BiO_3$ and blue for $Ba_{0.6}K_{0.4}BiO_3$. The samples were kept near liquid-nitrogen temperature during cleavage and measurements (with one exception[21]). Measurements were done on several samples of each composition. As will be shown in the next section, the surface qualities of the freshly cleaved samples were different in terms of oxygen and carbon related contaminations. This has to be due to intrinsic contamination in some of the crystals.

The photoemission and XAS measurements were performed at beamline 22 at the MAX national synchrotron radiation laboratory in Lund, Sweden. The beamline is equipped with a modified Zeiss SX-700 plane grating monochromator.[22] A Scienta-type hemispherical electron energy analyzer (200-mm mean radius) with a multichannel detector system[23] was used in the photoemission measurements. The total-energy resolution was dependent on the photon energy used and varied in the range 0.1 eV ($h\nu=95$ eV) through 0.5 eV ($h\nu=600$ eV). XAS spectra were measured by detecting the total electron yield using a channeltron. In the XAS measurements at the O *K* edge the photon energy resolution was 0.3 eV. The photoemission binding energy scale was determined with reference to the Fermi edge of a gold sample, whereas the absolute values of the photon energy scale in the XAS spectra were calibrated according to the procedure described in Ref. 24.

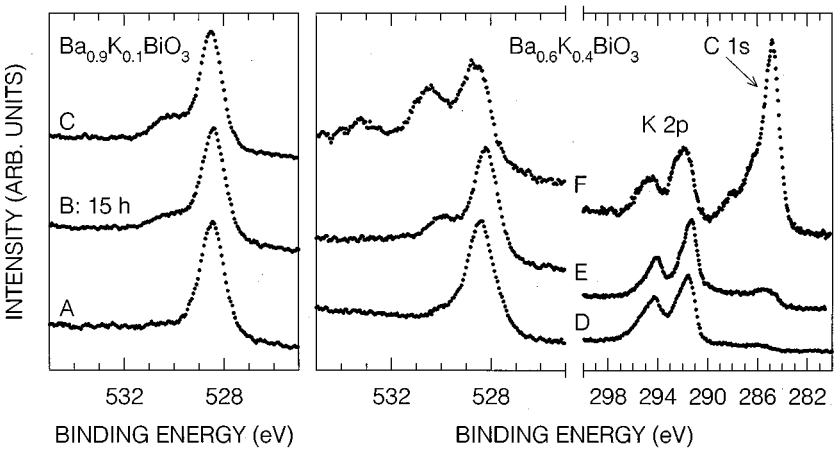

FIG. 1. O 1*s* photoemission spectra ($h\nu = 600$ eV) of two $Ba_{0.9}K_{0.1}BiO_3$ samples (left panel, *A*, *B*, and *C*; *B* is measured on the same sample as *A* but 15 h later) and three $Ba_{0.6}K_{0.4}BiO_3$ samples (right panel, *D*, *E*, and *F*). For the $Ba_{0.6}K_{0.4}BiO_3$ samples the C 1*s* and K 2*p* spectra ($h\nu = 440$ eV) are also shown, normalized to the K 2*p* intensity.

III. RESULTS AND DISCUSSION

A. Core-level photoemission spectra

Figure 1 shows O 1*s* photoemission spectra for $Ba_{0.9}K_{0.1}BiO_3$ (*A*,*B*,*C*) and $Ba_{0.6}K_{0.4}BiO_3$ (*D*,*E*,*F*). All spectra except *B* are measured on different samples directly after cleavage. Spectrum *B* is from the same sample as spectrum *A*, but measured after about 15 h in UHV. Also shown in Fig. 1 are the C 1*s* spectra for the $Ba_{0.6}K_{0.4}BiO_3$ samples. The O 1*s* intensity at and above 530 eV clearly scales with the C 1*s* intensity. From these data it is apparent that intense O 1*s* components with a higher binding energy (E_b) than the main peak at about 528.5 eV are of extrinsic nature. This is in sharp contrast to the previous suggestion[9] that these structures reflect different intrinsic oxidation states. For spectra *A*, *B*, and *C*, i.e., for $Ba_{0.9}K_{0.1}BiO_3$, the correlation of the feature at 530 eV to the C 1*s* intensity was less obvious because the C 1*s* intensity was in all these cases rather low. However, a small increase in the C 1*s* intensity was found as a function of time in UHV corresponding to spectra *A* and *B*. It is concluded from these spectra that clean $Ba_{0.9}K_{0.1}BiO_3$ is characterized by a single sharp O 1*s* peak as seen in spectrum *A*. The peak can be fitted with one symmetric voigt function. The small additional intensity above 530 eV can, at least partly, be assigned to the inelastic background of the main peak. However, spectrum *D* shows that clean $Ba_{0.6}K_{0.4}BiO_3$ does have some additional intensity on the high E_b side of the O 1*s* peak which is not present for $Ba_{0.9}K_{0.1}BiO_3$. The high E_b feature in spectrum *D* is not believed to be of extrinsic nature since this sample gave a very low C 1*s* intensity as seen in Fig. 1. Furthermore, the valence-band spectrum of the same sample did not show any traces of contamination (cf. Sec. III B).

The cation core-level photoemission data for $Ba_{0.9}K_{0.1}BiO_3$ ($x = 0.1$) and $Ba_{0.6}K_{0.4}BiO_3$ ($x = 0.4$) crystals having O 1*s* spectra similar to the best spectra *A* and *D* in Fig. 1 are displayed in Fig. 2. All the spectra in Fig. 2 were measured on the same two samples. Starting from the bottom of Fig. 2 it is obvious that the Bi 4*f* spectra of the two compounds are very different. The intensity on the high E_b side which gives rise to an asymmetric profile for $Ba_{0.9}K_{0.1}BiO_3$ is much more pronounced for $Ba_{0.6}K_{0.4}BiO_3$, in fact a clearly resolved shoulder is seen. The topmost Bi 4*f* spectrum is the same as spectrum *B* but numerically convoluted with a Gaussian profile with a width of 0.75 eV in order to resemble the energy resolution in a standard x-ray photoelectron spectroscopy (XPS) experiment. The line shape of this spectrum is similar to previous reported Bi 4*f* XPS spectra,[9,11,16] which clearly demonstrate the need for high-energy resolution ($\Delta E = 0.25$ eV for Bi 4*f* in the present measurements) in order to do detailed core-level studies of these compounds. It is also noted that the line shapes of the present Bi 4*f* spectra *A* and *B* are in qualitative agreement with the results of Nagoshi *et al.*,[15] who utilized monochromatized x rays ($\Delta E = 0.45$ eV) in their study of cleaved polycrystalline samples.

A fundamental question in the discussion of Bi core-level spectra of $Ba_{1-x}K_xBiO_3$ is the valence state of bismuth. In an ionic description of the parent compound, $BaBiO_3$, the bismuth valence is Bi^{4+}. It was suggested early[25] that $BaBiO_3$ contains Bi^{3+} and Bi^{5+} ions instead of Bi^{4+}, which are ordered on the inequivalent Bi sites of the monoclinically distorted lattice. In contrast to this proposition band-structure calculations[26] for monoclinic $BaBiO_3$ gave no significant difference between the valence charge densities of the inequivalent Bi sites. Furthermore, a Bi^{4+} valence has been proposed from XAS measurements at the Bi L_3 edge.[27] The chemical sensitivity of core-level spectroscopy could be able to resolve this question. Indeed, the line shape of spectra *A* and *B* in Fig. 2 could be interpreted as being dependent upon a various degree of bismuth valence mixing in the two compounds, but there exist some difficulties in establishing such an interpretation. First of all, the binding energy shift between Bi model compounds containing Bi^{3+} (Bi_2O_3) and Bi^{5+} ($NaBiO_3$) is negligibly small[15,28] as compared to the widths of the Bi 4*f* spectra in Fig. 2. In addition it should be noted that the binding energies of the low-energy peaks in spectra *A* and *B* are in the region between the values found for Bi and Bi_2O_3. Finally, inequivalent Bi sites are only expected for the semiconducting phase of $Ba_{1-x}K_xBiO_3$ whereas the metallic phase is cubic.[7,8] It is thus not possible to relate the Bi 4*f* line-shape changes between $Ba_{0.9}K_{0.1}BiO_3$ and $Ba_{0.6}K_{0.4}BiO_3$ in Fig. 2 to this structural difference. An alternative explanation for the Bi 4*f* line shape for $Ba_{0.6}K_{0.4}BiO_3$ is provided by the suggestion of Wagener *et al.*[11] that at least part of the intensity on the high E_b side of the core-level spectra for

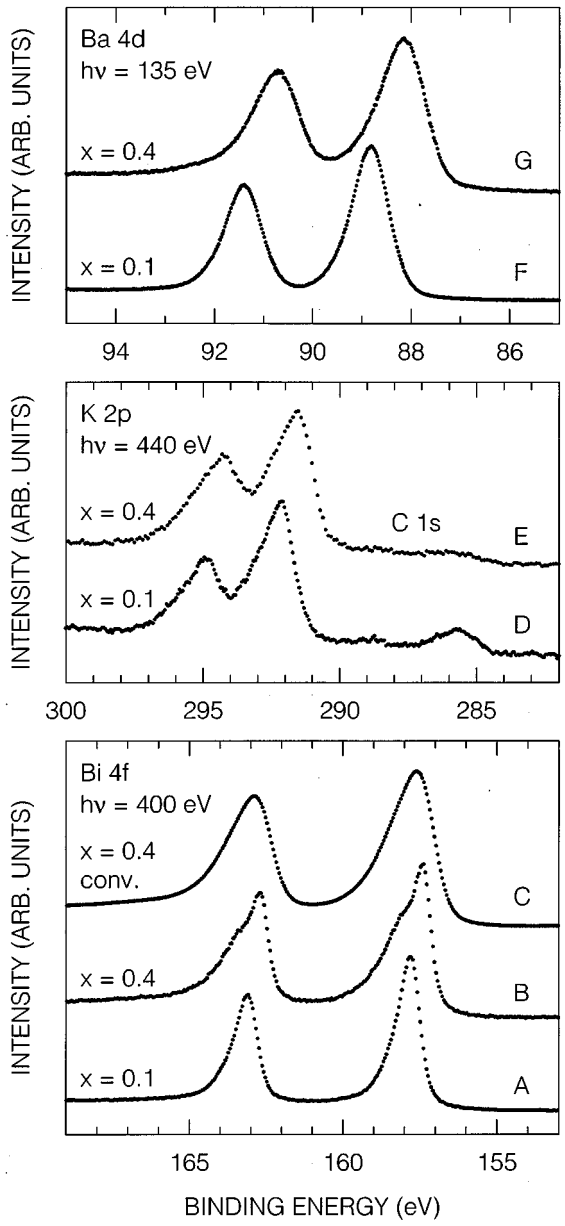

FIG. 2. Bi $4f$ (A, B, and C), K $2p$ (D and E), and Ba $4d$ (F and G) core-level photoemission spectra of $Ba_{0.9}K_{0.1}BiO_3$ ($x=0.1$) and $Ba_{0.6}K_{0.4}BiO_3$ ($x=0.4$). Spectrum C is the result of a convolution of spectrum B with a Gaussian profile with a width of 0.75 eV.

$Ba_{0.6}K_{0.4}BiO_3$ is due to an energy-loss structure. This possibility will be discussed further below.

Spectra D and E in Fig. 2 show the K $2p$ core level spectra as well as the C $1s$ region at lower energy. The C $1s$ emission is seen to be very weak for both compounds, the apparent larger C $1s$ intensity relative to the K $2p$ intensity for $Ba_{0.9}K_{0.1}BiO_3$ being mainly due to the lower potassium content in this sample. As for Bi $4f$, the K $2p$ line shape is asymmetric suggesting a structure on the high E_b side which is slightly more intense for $Ba_{0.6}K_{0.4}BiO_3$ as compared to $Ba_{0.9}K_{0.1}BiO_3$, but it is not as clearly resolved as in the Bi $4f$ spectrum.

At the top of Fig. 2 the Ba $4d$ core level spectra for the two compounds are shown. The trend of the line shape found

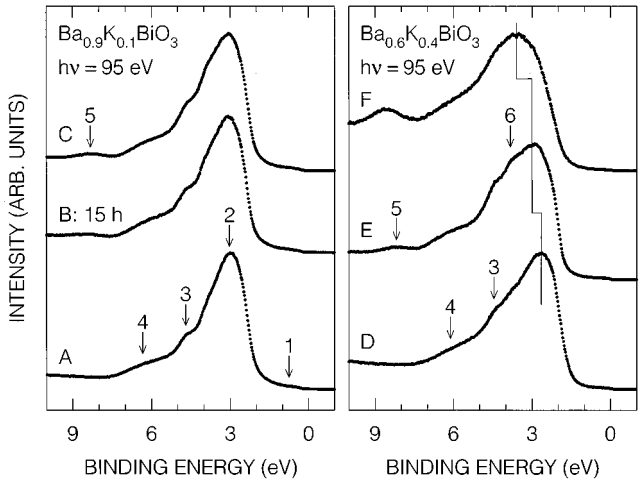

FIG. 3. Valence-band photoemission spectra of the same $Ba_{0.9}K_{0.1}BiO_3$ (left panel) and $Ba_{0.6}K_{0.4}BiO_3$ (right panel) samples as the corresponding spectra in Fig. 1.

from the Bi $4f$ and K $2p$ spectra are also seen in the Ba $4d$ spectra, i.e., the line shape is asymmetric with the larger asymmetry for $Ba_{0.6}K_{0.4}BiO_3$, but with the difference that no signs of a resolved feature at the high E_b side can be seen.

A common property of the core level data shown in Fig. 2, besides the asymmetry which will be discussed below, is the negative E_b shift for $Ba_{0.6}K_{0.4}BiO_3$ as compared to $Ba_{0.9}K_{0.1}BiO_3$. The magnitude of the shift of the core-level peak is smallest for Bi $4f$, 0.4 eV, and largest for Ba $4d$, 0.65 eV. O $1s$ spectra, measured on the same two samples as the cation spectra in Fig. 2, gave a similar type of shift, but with a smaller magnitude, 0.3 eV. In a recent study[16] of the doping dependency of the core-level binding energies in $Ba_{1-x}K_xBiO_3$ negative shifts as a function of increasing potassium content were interpreted to be largely due to a shift of the chemical potential. This interpretation explains parts of the shifts observed in the present study, but the differences in the shifts between the elements indicate that this is not the only contribution.

The asymmetric profiles seen for all spectra in Fig. 2 make it reasonable to assume that energy-loss structures contribute to the spectra as suggested by Wagener *et al.*[11] Concerning $Ba_{0.6}K_{0.4}BiO_3$ a plasmon energy of about 1.4–1.8 eV has been determined by optical measurements.[29] The high E_b structure in the core-level spectra of $Ba_{0.6}K_{0.4}BiO_3$ is shifted about 1 eV from the leading low-energy peak, a value slightly less than the predicted plasmon energy, but in reasonable agreement. The agreement is improved if the surface sensitivity of photoemission is considered which makes it possible that a surface plasmon having a lower energy than the bulk plasmon becomes important. For $Ba_{0.9}K_{0.1}BiO_3$ no asymmetry was found in the O $1s$ spectrum, indicating that energy losses do not affect the core-level line shapes for this semiconducting composition. It could be the case that the weak, as compared to $Ba_{0.6}K_{0.4}BiO_3$, asymmetries found for the cations core levels of $Ba_{0.9}K_{0.1}BiO_3$ are due to inequivalent sites in this distorted structure.

Although it appears to be well justified to assign the high E_b core-level spectral feature of $Ba_{0.6}K_{0.4}BiO_3$ to a plasmon

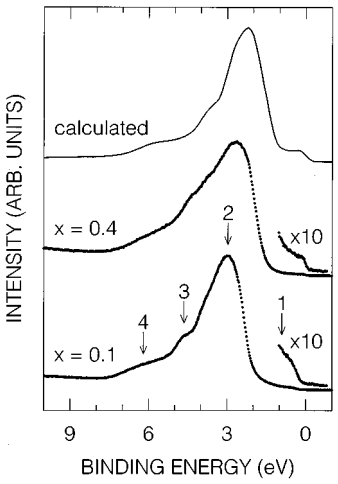

FIG. 4. Experimental valence-band photoemission spectra for $Ba_{0.9}K_{0.1}BiO_3$ ($x=0.1$) and $Ba_{0.6}K_{0.4}BiO_3$ ($x=0.4$) measured at 95-eV photon energy together with the calculated valence-band spectrum of Hamada *et al.* (Ref. 5), see text for details.

loss, another contribution must be considered because of the following reason. Core-level spectra measured on several crystals showed that the high E_b structure could be both more and less intense as compared to the spectra shown in Fig. 2, independent of the cleanliness of the surface (this effect is seen in the K $2p$ spectra in Fig. 1). This behavior indicates that some of the intensity in the high E_b shoulder of the core-level spectra arises from inhomogenities at the surfaces of the cleaved crystals which differ between the samples. This inhomogeneity could either be due to a disorder of the potassium distribution in the bulk, for instance by a microscopic phase separation, yielding different potassium concentration at the surface between different cleaved crystals, or arise from defects created by the cleavage. It appears reasonable to propose that the low E_b component of the core levels for $Ba_{0.6}K_{0.4}BiO_3$ is representative for the nominal composition whereas regions with lower potassium content could contribute to the intensity at higher E_b. An inspection of the binding energies of the core-level features for both types of samples in Fig. 2 reveals that this explanation is able to account for the high E_b features in the spectra of $Ba_{0.6}K_{0.4}BiO_3$.

B. Valence-band photoemisssion spectra

Figure 3 shows a set of valence-band spectra of the same samples as in Fig. 1. In spectra C,E, and F a feature (5) is seen at $E_b \approx 8.5$ eV which was found for some freshly cleaved samples. It is evident from the spectra in Figs. 3 and 1 that this feature is correlated to contaminations as measured by the O 1s and C 1s emissions. Spectra A and D have no such feature at all, whereas spectrum B shows that after about 15 h in UHV the 8.5 eV feature has become visible. From these findings it is concluded that clean $Ba_{1-x}K_xBiO_3$ is characterized by the absence of a structure above 8-eV E_b, when measured with a photon energy in the ultraviolet or soft x-ray regions. In XPS measurements an intrinsic feature can appear in this region due to the relatively higher cross section for Bi 6s,p states, as compared to O $2p$ states, for photon energies in the x-ray region.[5] In spectra E and F (and to a less degree in spectra B and C) it is seen how a consecutively higher degree of contamination makes structures 3 and 5 more intense and a new structure, 6, grows at 3.8 eV.[21] The enhancement of features 3 and 6 results in a broadening of the main valence-band peak which shifts towards higher E_b as marked by the broken line in Fig. 3. For the highly contaminated sample (spectrum F) the intensity in the vicinity of E_F is reduced as compared to clean $Ba_{0.6}K_{0.4}BiO_3$.

In order to emphasize the differences between the valence bands of $Ba_{0.9}K_{0.1}BiO_3$ and $Ba_{0.6}K_{0.4}BiO_3$ the spectra A and D of Fig. 3 are plotted on a common energy scale in Fig. 4. The most pronounced difference between the spectra for $Ba_{0.6}K_{0.4}BiO_3$ and $Ba_{0.9}K_{0.1}BiO_3$ is that the former shows a clear Fermi edge. Moreover, the valence-band features are to various degree shifted to lower E_b in $Ba_{0.6}K_{0.4}BiO_3$ and the intensity ratios between the main peak and features 3 and 4 are smaller than for $Ba_{0.9}K_{0.1}BiO_3$.

Figure 4 also shows the calculated photoemission spectrum of Hamada *et al.*[5] The theoretical spectrum is generated from the band structure for cubic $BaBiO_3$ calculated in the local-density approximation with a band filling corresponding to $x=0.29$ in $Ba_{1-x}K_xBiO_3$, i.e., a rigid-band model is used to represent metallic $Ba_{1-x}K_xBiO_3$. Hamada *et al.*[5] presented two calculated spectra for the ultraviolet-soft x-ray region corresponding to photon energies of 21.2 and 70 eV. In the present comparison the theoretical spectrum for a photon energy of 21.2 eV was chosen because the broadening used for this spectrum corresponds better to the energy resolution of the present experiment than the broadening used for the calculated 70-eV spectrum. Except for the different broadenings, there are no significant differences between the calculated 21.2- and 70-eV spectra. The intensity at these photon energies is predicted to be dominated by the oxygen partial density of states.

In the following discussion of the agreement between theoretical and experimental valence-band data the results from two other calculations will also be considered. The difference between those two calculations and the one displayed in Fig. 4 concerns mainly the way to handle the crystal structure and the stoichiometry. Mattheiss and Hamann[26] aimed to study the semiconducting mother-compound $BaBiO_3$ by using the experimentally determined monoclinic crystal structure in their band-structure calculation. Papaconstantopoulos *et al.*[6] used a tight-binding approach to study the effect from potassium substitution in more detail than what is possible in the rigid-band model used by Hamada *et al.*[5]

From the spectra in Fig. 4 a detailed comparison between experimental and calculated band-structure results can be made. First it is noted that the overall shape of the experimental spectra agrees well with the band theory result. All features 1–4 in the experimental spectra are recognized in the theoretical spectrum and can be identified according to the density of states calculations as follows. At the top of the valence band (1) is the antibonding Bi 6s-O $2p$ band which crosses the Fermi level in the metallic samples. The main

valence band intensity (2) at about 3 eV as well as feature 3 is due to nonbonding O $2p$ states, the latter with a predicted small Ba $6s$ contribution. Feature 4 consists of the bonding O $2p$ and Bi $6p$ states whereas the bonding counterpart of feature 1 results in a broad and flat structure at higher E_b. As expected from a rigid-band behavior, E_b of the main features in the experimental spectrum of $Ba_{0.6}K_{0.4}BiO_3$ is in better agreement with the calculated spectrum than the results for $Ba_{0.9}K_{0.1}BiO_3$. However, it is clear from Fig. 4 that also for $Ba_{0.6}K_{0.4}BiO_3$ the main valence-band features are shifted to higher E_b as compared to the calculated spectrum.

Although there is a general good agreement between the theoretical and experimental valence band results in Fig. 4, some discrepancies indicate that the rigid-band model used in the calculation is not able to describe the metallic phase of $Ba_{1-x}K_xBiO_3$ accurately in all details. First, it is evident from the spectra in Fig. 4 that the relative intensities of the features in the experimental spectrum of $Ba_{0.9}K_{0.1}BiO_3$ are in better agreement with the calculated spectrum than the results for $Ba_{0.6}K_{0.4}BiO_3$. Second, the experimental valence-band spectra do not show a rigid shift. A closer inspection of the experimental spectra in Fig. 4 shows that the change between the two spectra is better described as a stretch of the spectrum for $Ba_{0.6}K_{0.4}BiO_3$ towards lower E_b rather than a rigid shift, i.e., the top of the main valence band of $Ba_{0.6}K_{0.4}BiO_3$ is shifted about 0.4 eV towards lower E_b as compared to $Ba_{0.9}K_{0.1}BiO_3$, but the bottom of the two valence bands are at nearly the same position. These findings are in agreement with the band-structure results of Papaconstantopoulos *et al.*[6] who went beyond the rigid-band model to calculate the density of states for $Ba_{0.6}K_{0.4}BiO_3$. As compared to their results for $BaBiO_3$ they found that the position of E_F followed a rigid-band behavior, but the shape of the oxygen dominated density of states showed small differences resulting in an increase in the and width of about 0.4 eV for $Ba_{0.6}K_{0.4}BiO_3$.

A further difference between the theoretical band structure result and the experimental results in Fig. 4 concerns the intensity near E_F. First, a comment is needed to be made on the lack of a Fermi edge for $Ba_{0.9}K_{0.1}BiO_3$ which is in agreement with the semiconducting property of this composition. The model used to generate the theoretical spectrum in Fig. 4 results in a Fermi edge also for lower potassium concentrations corresponding to the semiconducting phase of $Ba_{1-x}K_xBiO_3$. This discrepancy should not be taken as evidence for limitations in the validity of band-structure calculations for $Ba_{1-x}K_xBiO_3$ in general. Indeed, an early and more comprehensive calculation for $BaBiO_3$, in which the monoclinic distortion of this structure was taken into account, showed a splitting of the bands around E_F consistent with the semiconducting property.[26] As noted previously, $Ba_{0.9}K_{0.1}BiO_3$ is distorted in a similar way.[7,8] For $Ba_{0.6}K_{0.4}BiO_3$, which has the cubic structure, the calculational scheme used by Hamada *et al.*[5] is expected to be a good approximation. However, it is seen in Fig. 4 that there is a lower photoemission intensity in the experimental spectrum for $Ba_{0.6}K_{0.4}BiO_3$ between E_F and $E_b \approx 1$ eV than in the calculated spectrum. This result indicates that this type of calculation is not able to correctly predict the density of states at E_F in superconducting $Ba_{1-x}K_xBiO_3$. However, in the light of the experience of valence-band photoemission in the 1:2:3-type cuprate HTSC,[30] for which it was found that the intensity at E_F was dependent on oxygen loss if the sample was not cooled to temperatures below 80 K, it is evident that the present deviation between experiment and theory needs to be confirmed by further studies. Most interesting are valence-band measurements of $Ba_{0.6}K_{0.4}BiO_3$ with varying oxygen content in the samples and the temperature dependence of the valence-band intensity at E_F for sample temperatures below the one used in the present experiment.

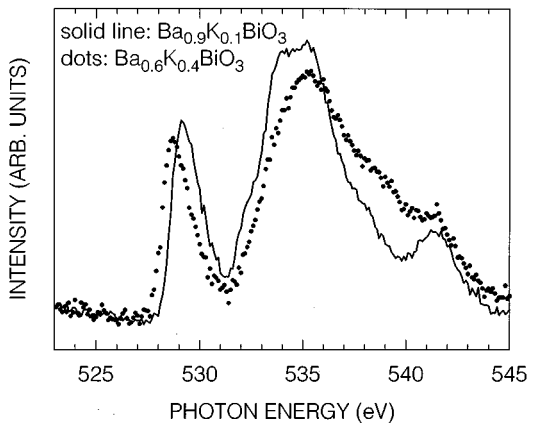

FIG. 5. XAS spectra at the O K edge for $Ba_{0.9}K_{0.1}BiO_3$ (solid line) and $Ba_{0.6}K_{0.4}BiO_3$ (dots). The spectra are normalized to the integrated intensity of the absorption up to 545 eV.

C. O *K*-edge x-ray-absorption spectra

For the hole-doped cuprate HTSC $YBa_2Cu_3O_{6+x}$,[31] $La_{2-x}Sr_xCuO_4$ (Ref. 32), and $Bi_2Sr_2Ca_{1-x}Y_xCu_2O_8$ (Ref. 33) it is well known that the intensity of a clearly resolved prepeak in the O K-edge XAS or EELS spectrum scales with the hole doping. The common interpretation of this behavior is that holes are created in O $2p$ states in the Cu-O_2 layers of the doped systems which leads to metallic properties. Figure 5 shows the total electron yield XAS spectra for the two types of $Ba_{1-x}K_xBiO_3$ crystals studied. These spectra display the local unoccupied p density of states of the core ionized oxygen. Most important to note in the spectra in Fig. 5 is that no additional prepeak occurs in metallic $Ba_{0.6}K_{0.4}BiO_3$ as compared to semiconducting $Ba_{0.9}K_{0.1}BiO_3$. The differences between the XAS spectra of the two types of crystals are instead some redistributions of the intensity between the different spectral features and a small shift of the absorption edge towards lower energy in the metallic system. In a previous O K-edge XAS study of $Ba_{1-x}K_xBiO_3$ the low-energy absorption peak seen at about 529 eV in the spectra in Fig. 5 was taken as an evidence for hole doping of oxygen with increasing potassium content.[8,34] However, it must be noted that this structure exists and is intense in the semiconducting phase, as is seen in the spectrum for $Ba_{0.9}K_{0.1}BiO_3$ in Fig. 5 and in the reported spectra for $BaBiO_3$.[8,35] If this absorption peak would correspond to doping-induced oxygen holes in a similar manner as for the cuprate HTSC it should be absent or strongly reduced for

these compositions as compared to the metallic phase. These facts indicate that the transition to the metallic phase of $Ba_{1-x}K_xBiO_3$ is of a different nature than that of hole-doped cuprate HTSC. The difference found between the O K-edge results for $Ba_{1-x}K_xBiO_3$ and the hole-doped cuprate HTSC is in agreement with the inverse photoemission resonance study of Wagener *et al.*,[11] who found an enhancement corresponding to O $2p$ holes near E_F for cuprate HTSC but no such behavior for $Ba_{0.6}K_{0.4}BiO_3$.

From above considerations it is concluded that the spectra in Fig. 5 provide no support for the notion that the metallic phase of $Ba_{1-x}K_xBiO_3$ is related to doping-induced holes in O $2p$ states at E_F as has been established for the hole-doped cuprate HTSC mentioned above. For the other bismuthate superconductor system $BaPb_{1-x}Bi_xO_3$ de Groot *et al.*[35] found that the O K-edge XAS spectra revealed a similar doping dependence as is found for $Ba_{1-x}K_xBiO_3$ in the present work, i.e., the edge structure showed a small shift as a function of the bismuth content and no additional prepeak was seen in the metallic regime. But the results for $BaPb_{1-x}Bi_xO_3$ are contradictory since Lin *et al.*[36] found an additional preedge structure for $BaPb_{0.75}Bi_{0.25}O_3$ and $BaPb_{0.5}Bi_{0.5}O_3$ as compared to $BaPbO_3$. The reason for this inconsistency in the results from $BaPb_{1-x}Bi_xO_3$ is not clarified.

To conclude this section some further aspects of the doping behavior of $Ba_{1-x}K_xBiO_3$ will be discussed. A hypothetical description of metallic $Ba_{1-x}K_xBiO_3$ as being doped with O $2p$ holes would be related to the fact that with fixed cation valences substitution of Ba^{2+} by K^{1+} implies the creation of oxygen holes, a description analogous to the case when La_2CuO_4 is doped with strontium. Such a description for the cuprate HTSC relies on the fact that the band gap of the insulating mother compounds is of the charge-transfer type which, due to the strong electron correlation in these materials, is believed to exist also in the metallic compounds.

For $Ba_{1-x}K_xBiO_3$, which does not have any valence band d or f states, no strong electron correlation is expected, a property which suggests that band-structure calculations should be able to give an adequate description of the electronic structure of this system. As noted above, the semiconducting regime of $Ba_{1-x}K_xBiO_3$ has been related to the distortion of the crystal structure which results in a band splitting around E_F. For the cubic phase, which corresponds to the metallic compositions of $Ba_{1-x}K_xBiO_3$, the band-structure results show that a single band crosses E_F. This band is less than half-filled due to the lower band filling in $Ba_{1-x}K_xBiO_3$ as compared to $BaBiO_3$.[37] Accordingly, n-type carriers are expected for metallic $Ba_{1-x}K_xBiO_3$, in agreement with the result from Hall measurements.[20] In the intermediate doping range $0<x<0.3$ the band filling of the semiconducting $Ba_{1-x}K_xBiO_3$ is progressively reduced until a critical doping level ($x=0.3$) is reached.[38] At $x=0.3$ the energy gained by the distortion of the crystal structure is lost and a crystallographic phase transition occurs to the metallic cubic phase.[38] This doping behavior is consistent with the assignment of the x-dependent core-level shifts of $Ba_{1-x}K_xBiO_3$ to a shift of the chemical potential. These observations imply that the semiconductor-metal transition is due to a closing of a band gap which is related to the corresponding crystallographic phase transition. No obvious argument against this description is found from the experimental results presented in this work since the valence-band spectra were found to be in qualitative good agreement with the band-structure results and no evidence was found from the XAS spectra for doping-induced oxygen holes in the metallic phase. In addition, the results of optical measurements have been found to be consistent with this explanation for the semiconductor-metal transition in $Ba_{1-x}K_xBiO_3$.[38,39] However, a modified description of the electronic structure of $Ba_{1-x}K_xBiO_3$ has also been proposed in which a dynamical lattice distortion exists in the metallic phase resulting in a band splitting around E_F.[16] It has been suggested[16] that this effect could account for the differences in intensity seen between the theoretical band structure and the experimental valence-band data in the vicinity of E_F. As pointed out in the previous section, further valence-band photoemission studies are needed to clarify this point.

IV. SUMMARY

Several aspects of the electronic structure of semiconducting $Ba_{0.9}K_{0.1}BiO_3$ and superconducting $Ba_{0.6}K_{0.4}BiO_3$ have been studied by valence and core-level photoemission as well as O K-edge XAS. The general shape of the valence-band spectra was found to agree to a large extent to the prediction from band-structure calculations. However, some discrepancies indicate that a theoretical representation of metallic $Ba_{1-x}K_xBiO_3$ by a rigid-band model applied to the calculated band structure for cubic $BaBiO_3$ is too simple to accurately describe the electronic structure of the metallic phase in detail. The XAS results showed that the metallic phase is not related to the presence of doping induced O $2p$ holes. This property of $Ba_{1-x}K_xBiO_3$ shows that the transition to the metallic phase is of a different nature as compared to that of the hole-doped cuprate HTSC. The core-level photoemission spectra for $Ba_{0.9}K_{0.1}BiO_3$ showed a small asymmetry for the cations which could tentatively be related to inequivalent sites in this distorted crystal structure. For $Ba_{0.6}K_{0.4}BiO_3$ the core-level spectra, in particular for bismuth, showed considerably more complicated line shapes than what could be expected from the cubic structure. This effect for $Ba_{0.6}K_{0.4}BiO_3$ was suggested to arise from a plasmon loss feature and a possible inhomogeneity at the surface. Clearly, more studies are needed to provide a better understanding of these core-level spectral line shapes.

ACKNOWLEDGMENTS

This work was supported by the Swedish Natural Science Research Council, the Swedish Research Council for Engineering Sciences, the Royal Swedish Academy of Science and the New Energy and Industrial Technology Development Organization (NEDO) in Japan. Support was also received from the Russian State Program on HTSC (Project No. 93160) and by a grant from the International Science Foundation (Project No. JBZ-100).

*Present address: Materials Physics, Department of Physics, Royal Institute of Technology, S-100 44 Stockholm, Sweden.

[1] See, for instance, W. E. Pickett, Rev. Mod. Phys. **61**, 433 (1989).

[2] L. F. Mattheiss, E. M. Gyorgy, and D. W. Johnson, Phys. Rev. B **37**, 3745 (1988).

[3] R. J. Cava, B. Batlogg, J. J. Krajewski, R. Farrow, L. W. Rupp, Jr., A. E. White, K. Short, W. F. Peck, and T. Kometani, Nature **332**, 814 (1988).

[4] L. F. Mattheiss and D. R. Hamann, Phys. Rev. Lett. **60**, 2681 (1988).

[5] N. Hamada, S. Massida, A. J. Freeman, and J. Redinger, Phys. Rev. B **40**, 4442 (1989).

[6] D. A. Papaconstantopoulos, A. Pasturel, J. P. Julien, and F. Cyrot-Lackmann, Phys. Rev. B **40**, 8844 (1989).

[7] S. Pei, J. D. Jorgensen, B. Dabrowski, D. G. Hinks, D. R. Richards, A. W. Mitchell, J. M. Newsam, S. K. Sinha, D. Vaknin, and A. J. Jacobson, Phys. Rev. B **41**, 4126 (1990).

[8] S. Salem-Sugui, Jr., E. E. Alp, S. M. Mini, M. Ramanathan, J. C. Campuzano, G. Jennings, M. Faiz, S. Pei, B. Dabrowski, Y. Zheng, D. R. Richards, and D. G. Hinks, Phys. Rev. B **43**, 5511 (1991).

[9] M. S. Hegde, P. Barboux, C. C. Chang, J. M. Tarascon, T. Venkatesan, X. D. Wu, and A. Inam, Phys. Rev. B **39**, 4752 (1989).

[10] M. W. Ruckman, D. Di Marzio, Y. Jeon, G. Liang, J. Chen, M. Croft, and M. S. Hegde, Phys. Rev. B **39**, 7359 (1989).

[11] T. J. Wagener, H. M. Meyer III, D. M. Hill, Yongjun Hu, M. B. Jost, J. H. Weaver, D. G. Hinks, B. Dabrowski, and D. R. Richards, Phys. Rev. B **40**, 4532 (1989).

[12] Y. Jeon, G. Liang, J. Chen, M. Croft, M .W. Ruckman, D. Di Marzio, and M. S. Hegde, Phys. Rev. B **41**, 4066 (1990).

[13] M. Nagoshi, Y. Fukuda, T. Suzuki, K. Ueki, A. Tokiwa, M. Kikuchi, Y. Syono, and M. Tachiki, Physica C **185-189**, 1051 (1991).

[14] R. Itti, I. Tomeno, K. Ikeda, K. Tai, N. Koshizuka, and S. Tanaka, Phys. Rev. B **43**, 435 (1991).

[15] M. Nagoshi, T. Suzuki, Y. Fukuda, K. Ueki, A. Tokiva, M. Kikichi, Y. Syono, and M. Tachiki, J. Phys. Condens. Matter **4**, 5769 (1992).

[16] H. Namatame, A. Fujimori, H. Torii, T. Uchida, Y. Nagata, and J. Akimitsu, Phys. Rev. B **50**, 13 674 (1994).

[17] M. L. Norton, Mater. Res. Bull. **24**, 1391 (1989).

[18] W. D. Mosley, J. W. Dykes, P. Klavins, R. N. Shelton, P. A. Sterne, and R. H. Howell, Phys. Rev. B **48**, 611 (1993).

[19] Y. Idemoto, Y. Iwata, and K. Fueki, Physica C **222**, 257 (1994).

[20] S. F. Lee, J. Y. T. Wei, H. Y. Tang, T. R. Chien, M. K. Wu, and W. Y. Guan, Physica C **209**, 141 (1993).

[21] Spectra *F* in Figs. 1 and 3 are measured on a sample having a different history than the others. The sample was first cleaved while it was kept cool by liquid nitrogen. It was then left in UHV for about 20 h until it was scraped with a diamond file at room temperature prior to measurements, which also were performed at room temperature. The freshly cleaved sample showed also the additional valence-band features seen in spectrum *F* in Fig. 3, but with a slightly different intensity distribution.

[22] R. Nyholm, S. Svensson, J. Nordgren, and A. Flodström, Nucl. Instrum. Methods A **246**, 267 (1986).

[23] J. N. Andersen, O. Björneholm, A. Sandell, R. Nyholm, J. Forsell, L. Thånell, A. Nilsson, and N. Mårtensson, Synch. Rad. News **4**(4), 15 (1991).

[24] M. Qvarford, N. L. Saini, J. N. Andersen, R. Nyholm, E. Lundgren, I. Lindau, J. F. van Acker, L. Leonyuk, S. Söderholm, and S. A. Flodström, Physica C **214**, 119 (1993).

[25] D. E. Cox and A. W. Sleight, Solid State Commun. **19**, 969 (1976).

[26] L. F. Mattheiss and D. R. Hamann, Phys. Rev. B **28**, 4227 (1983).

[27] J. B. Boyce, F. G. Bridges, T. Claeson, T. H. Geballe, and J. M. Remeika, Phys. Rev. B **41**, 6306 (1990).

[28] W. E. Morgan, W. J. Stec, and J. R. Van Wazer, Inorg. Chem. **12**, 953 (1973).

[29] I. Bozovic, J. H. Kim, J. S. Harris, Jr., E. S. Hellman, E. H. Hartford, and P. K. Chan, Phys. Rev. B **46**, 1182 (1992).

[30] R. S. List, A. J. Arko, Z. Fisk, S-W. Cheong, S. D. Conradson, J. D. Thompson, C. B. Pierce, D. E. Peterson, R. J. Bartlett, N. D. Shinn, J. E. Schirber, B. W. Veal, A. P. Paulikas, and J. C. Campuzano, Phys. Rev. B **38**, 11 966 (1988).

[31] P. Kuiper, G. Kruizinga, J. Ghijsen, M. Grioni, P. J. W. Weijs, F. M. F. de Groot, G. A. Sawatsky, H. Verweij, L. F. Feiner, and H. Petersen, Phys. Rev. B **38**, 6483 (1988).

[32] N. Nücker, J. Fink, B. Renker, D. Ewert, C. Politis, P. J. W. Weijs, and J. C. Fuggle, Z. Phys. B **67**, 9 (1987).

[33] H. Matsuyama, T. Takahashi, H. Katayama-Yoshida, T. Kashiwakura, Y. Okabe, S. Sato, N. Kosugi, A. Yagishita, K. Tanaka, H. Fujimoto, and H. Inokuchi, Physica C **160**, 567 (1989).

[34] It is noted that the general shape of the O *K*-edge spectra in the present study is similar to the results of Ref. 8, but the entire energy scale is shifted about 4 eV in the earlier study.

[35] F. M. F. de Groot, J. C. Fuggle, and J. M. van Ruitenbeek, Phys. Rev B **44**, 5280 (1991).

[36] C. L. Lin, S. L. Qiu, J. Chen, M. Strongin, G. Cao, C.-S. Jee, and J. E. Crow, Phys. Rev. B **39**, 9607 (1989).

[37] See Ref. 4. $BaBiO_3$ gives a half-filled band at E_F in the cubic phase.

[38] This description of the doping behavior of $Ba_{1-x}K_xBiO_3$ and its agreement with the results from optical measurements are discussed in detail in M. A. Karlow, S. L. Cooper, A. L. Kotz, M. V. Klein, P. D. Han, and D. A. Payne, Phys. Rev. B **48**, 6499 (1993).

[39] H. Sato, S. Tajima, H. Takagi, and S. Uchida, Nature **338**, 241 (1989).